

VISUALIZATION OF SUPERSONIC FLOWS IN SHOCK TUNNELS, USING THE BACKGROUND ORIENTED SCHLIEREN TECHNIQUE

Sreekanth Raghunath*, David. J. Mee[#], Thomas Roesgen[§], Peter. A. Jacobs[¶]
The Centre for Hypersonics,
The University of Queensland, Brisbane, Australia 4072

Abstract

Visualisation of supersonic compressible flows using the Background Oriented Schlieren (BOS) technique is presented. Results from experiments carried out in a reflected shock tunnel with models of a 20° semi-vertex angle circular cone and a re-entry body in the test section are presented. This technique uses a simple optical set-up consisting of a structured background pattern, an electronic camera with a high shutter speed and a high intensity light source. Tests were conducted with a Mach 4 conical nozzle, with nozzle supply pressure of 2 MPa and nozzle supply temperature of 2000 K respectively. The images captured during the test were compared using PIV style image processing code. The intensity of light at each point in the processed image was proportional to the density at that point. Qualitative visualization of shock shapes, with images clearly indicating regions of subsonic and supersonic flows was achieved. For the cone, the shock angle measured from the BOS image agreed with theoretical calculations to within 0.5°. Shock standoff distances could be measured from the BOS image for the re-entry body.

Introduction

Visualisation of density fluctuations has long been used to assist with the understanding of flows in density-stratified systems. Most of the techniques for this purpose use the relationship between the refractive index and the density of the fluid to determine the density fluctuations in the flowfield.

A novel technique has been used to visualize flow in a shock tunnel. The Background Oriented Schlieren technique uses digital image processing, which replaces the optical processing present in the classical schlieren. In its most basic form, this technique uses an electronic camera with high shutter

speed, a high intensity light source and a structured background dot pattern as the primary optical elements for experimentation.

The experiments were performed in the Drummond shock tunnel at The University of Queensland. To the authors' knowledge, there are no previously published papers in which this technique has been used in shock tunnels.

The BOS technique

Background-Oriented Schlieren (BOS) is a fast and emerging technique for the visualisation of high speed flows as well as flows in general. The use of simple optics, the high accuracy, the fast evaluation, the governing role of numerical methods are some of the major advantages of using this method¹.

In a simple realization of the BOS setup (see Figure 1), a structured pattern located in the background of a flow of interest is recorded as a digital image. The density gradients present in the inhomogeneous flow region induce some distortion in what the camera sees, compared to when there is a homogeneous field present in between the camera and the background pattern. An image of the undistorted background pattern is taken as an additional recording, in order to perform deconvolution of the two images to derive information about the inhomogeneous transfer channel under consideration.

The BOS technique is also known as 'computerized' or 'synthetic' schlieren technique. As a tool for determining the density distributions in the flow, this technique has been applied previously for numerous applications: measurement of aircraft wakes and vortices in airports¹, field tests of helicopters to measure rotor flow, and in the measurement of density gradients produced by combustion and heaters². The performance of the BOS technique was experimentally determined and the accuracy of experimental density ratio measurements has been found to be within 3% of theoretical levels³.

For the current work, involving visualisation of density variations in a supersonic shock tunnel, the basic principles of BOS have been used. The basic optics used for a BOS setup and how these can be used to obtain qualitative and quantitative measurements are discussed by Dalziel et al⁴. A

* Graduate Student and presenting author, AIAA student member.

[#] Associate Professor, AIAA senior member.

[§] Professor, Institute of Fluid Dynamics, ETH Zurich, Switzerland, visiting UQ from Oct 2003 – Apr 2004, AIAA senior member.

[¶] Senior Lecturer, AIAA senior member.

discussion regarding the sensitivity of the technique to the distances between the background pattern, the inhomogeneous flow field and the camera are discussed by Dalziel et al⁵.

The Gladstone Dale equation^{6, 7} gives a relationship between the refractive index of a medium and its density. If n represents the refractive index and ρ indicates the density of the fluid in the medium, the relation between them is given by

$$n-1 = K * \rho,$$

where K is a constant called the Gladstone Dale constant. The Gladstone Dale constant depends on the characteristics of the gas in the medium and weakly on the frequency of light used. Typical values of the Gladstone Dale constant for different gases can be found in Merzkirch⁶.

Knowing the relationship between the fluid density and its refractive index, the problem of how a light ray is disturbed in an inhomogeneous refractive field has been previously investigated⁶. Physical phenomena like diffraction and dispersion were excluded from the analysis.

A comprehensive review of the principles and applications of the Particle Image Velocimetry (PIV) is presented by Raffel et al⁸. An introduction to digital PIV by Willert and Gharib⁹ provides a lucid description of the computerized form of the original PIV technique.

The digital PIV technique is a two-dimensional technique, involving the computational analysis of digitally recorded images. It removes both the photographic and opto-mechanical processing steps inherent to the normal PIV technique. Two sequential images are sub-sampled at one particular area via an interrogation window. Within these image samples, an average spatial shift of particles may be observed from one sample to its counterpart in the other image, provided a flow is present in the illuminated plane. One of the sampled regions is considered as input to a system whose output corresponds to the sampled region of the other image recorded at a later time.

One conceivable way of recovering the spatial displacement function is via a de-convolution technique. The displacement function needs to be measured to sub-pixel accuracy to achieve sufficient resolution in the particle displacement values. A statistical technique called spatial cross correlation is used to find the displacement function to sub pixel accuracy. A high cross correlation value near 1 is observed where many particle images match up with their corresponding spatially shifted partners. The highest cross correlation peak is considered to represent the best match of particle images. Fast Fourier transforms simplify and significantly speed

up the cross correlation process^{10, 11}. Rather than performing a sum over all the elements of the sampled region for each element, the operation can be reduced to a complex conjugate multiplication of each corresponding pair of Fourier coefficients. Another approach, using a filtered back projection algorithm has been suggested by Venkatakrishnan and Meier¹².

Improvements have been suggested in deriving a better correlation by improving the cross correlation method for digital PIV¹³, error correction using a correlation based correction (CBC) technique¹⁴ and optimal sub-pixel interpolation techniques to derive a sub-pixel accurate correlation peak position¹⁵.

Experimental setup

The Drummond reflected shock tunnel at The University of Queensland was used for all experiments reported here. The Drummond tunnel consists of a driver section, which was filled with helium. The driver was separated from the driven section or the shock tube by means of a 0.6 mm thick aluminium primary diaphragm. The driver section of the tunnel has a solenoid-actuated piercer used to rupture the primary diaphragm. The shock tube was filled with a test gas of air to 15 kPa.

A Mach 4 conical nozzle was fitted at the end of the shock tube, which leads into the dump tank¹⁶. The dump tank was evacuated to a pressure of approximately 400 Pa before the shot. The nozzle was sealed at the throat by a 0.025 mm thick cellophane secondary diaphragm. This secondary diaphragm maintains the pressure difference between the shock tube and dump tank prior to the shot. The test object was placed in the dump tank. The test section had multiple optical access in the form of glass windows on both the sides and the top and bottom of the test volume, which made it convenient for flow visualization.

The conditions at the stagnation point and at the nozzle exit plane have been calculated using a software package, called STN¹⁷. This code is quasi one-dimensional and models the shock compression of the test gas in the shock tube and the expansion of the test gas through the nozzle using equilibrium chemistry. STN requires as inputs the filling pressure and temperature of the test gas in the shock tube, the measured speed of the shock wave along the shock tube, the measured nozzle supply pressure and the area ratio of the nozzle.

The nozzle supply pressure and temperature for the test case considered here are presented in Table 1.

Table 1: Experimental flow conditions

Shock tube fill pressure, p_1	15 kPa
Reservoir pressure, p_4	3.2 MPa
Stagnation pressure, p_0	2 MPa
Stagnation temperature, T_0	2000 K
Stagnation enthalpy, h_0	2.25 MJ/kg

Two test objects were mounted in the test section in the Drummond tunnel. The first one was a 20° semi-vertex angle circular cone of axial length 37.6 mm. This model was sting mounted in the test section, with the tip of the cone at a distance of 12 mm from the exit plane of the nozzle. This simple model was chosen so that the shock angles could be compared with theoretical and computational results.

The second object was a model of the Muses C re-entry capsule. The Muses-C re-entry capsule was designed for an asteroid sample return mission¹⁸. The geometry for the Muses-C entry capsule is a sphere-cone shape having a nose radius of 200 mm, a cone angle of 45° and a base diameter of 400 mm. The prototype used for the current work was a 1:10 scale model of the flight vehicle. A bow shock is formed when a supersonic flow impinges on to this geometry at a zero angle of attack, with subsonic flow regions between the shock and the body. The tip of this model was located at a distance of 25 mm from the exit plane of the nozzle and the model was sting mounted in the test section.

For the present work, a Scorpion IEEE-1394 digital camera (Model – SCOR20SO) from Point Grey Research Inc. was used for recording the images. This camera uses a black and white version of the Sony 1/1.8" CCD sensor (model ICX274 sensor). The sensor is of interline progressive scan type, which means that the sensor records an entire image frame at once. The sensor has a maximum resolution of 1600 x 1200 pixels. It was placed at a distance of 0.7 m from the test flow region (see Figure 1).

The camera provides an option of a large range of exposure durations, starting from 110 μ s and extending to a maximum of 12285 ms. For the present work, the camera was operated with a 200 μ s exposure. The camera was triggered by the arrival of the primary shock wave at the end of the shock tube as detected by a pressure transducer located 75 mm upstream of the nozzle end of the shock tube. An appropriate delay time was included so that the camera's shutter remained open for 200 μ s during the period of steady test flow over the model in the test

section. The images were downloaded directly onto the hard disk of the computer, through a 6-pin IEEE 1394 interface.

The light source used to illuminate the structured pattern was a xenon stroboscope (Movistrob 400, manufactured by Bamberg & Bormann Electronic GmbH), which was placed at a distance of 0.7 m behind the background pattern. This stroboscope is rated at a maximum light intensity of 550 lux (or lumens/m²), with a pulse width of about 8 μ s. It had an inherent delay of about 25 μ s to an external trigger, and this had to be taken into account while synchronizing the flash with the camera and the establishment of the flow.

The other important optical element required by this method is a structured pattern, to be placed in the background of the region of inhomogeneity. The Drummond shock tunnel has windows on the sides of the test section, which are 0.11 m in diameter. For the current work, the pattern was placed in one of the windows. The structured pattern was back-illuminated using the light source (see Figure 1).

The size of the dots in the pattern, 0.3 mm in diameter in this case, was such that the lens on the camera could resolve the pattern with the smallest feature being 2 pixels wide. The pattern should have a high contrast, preferably of black and white regions. The size of the features depends upon the imaging geometry, camera capabilities as well as the flow conditions in the inhomogeneous medium.

The structured background pattern was generated using a random number generator code, which places the dots in the pattern in such a way that autocorrelation of the features of the pattern should approach a delta function. The random number generator generates a two dimensional array, containing in it the co-ordinates of the dots in the dot pattern. This array of dots is distributed in the pattern in such a way that, no dot is placed in a region occupied by a 3*3 pixel grid surrounding any other dot. For the current work, the pattern thus generated was printed out on a transparency with a laser-jet printer. The pattern generated can be seen in the background of Figures 2a and 3a.

The pressure at the end of the shock tube was measured using a PCB model 111A26 piezoelectric pressure transducer. The transducer was located 75 mm from the nozzle end of the shock tube. A thin film heat transfer gauge was located 220 ± 1 mm further upstream from the pressure transducer. The heat transfer gauge was used just as a shock timing station, whereas the pressure transducer was used as the second component of the shock timing instrumentation and was used to measure the nozzle supply pressure.

A digital oscilloscope (model TDS2014 from Tektronix) was used to record the voltage outputs from the pressure transducer and the thin film heat transfer gauge. The shock speed was calculated from the voltage versus time plots generated, by measuring the time between when the primary shock went past the two shock timing stations.

A delay generator (model SRS-DG535 from Stanford Research Systems) was used for the current work. The delay generator was triggered by the signal from the pressure transducer. Knowing the shock speed, the conditions at the nozzle supply region and the flow conditions at the exit of the nozzle, the time between when the pressure transducer sensed the shock and when the test flow was established over the test object was calculated. This calculated delay time was used to control the opening of the shutter of the electronic camera as well as the flashing of the stroboscope.

Results and discussion

As mentioned earlier, a set of digital image processing steps was applied to the two images captured during the experiments. The post-processing of the images from the shots was carried out using the Matlab Image Processing Toolbox. Computerized image processing is one of the most important advantages of the BOS technique. It reduces the time taken for comparing the images, both by eliminating the photographic and opto-mechanical processing of the images as well as by adopting numerical techniques to analyze the images. The reference image (see Figures 2a and 3a), which is the one taken with no flow in the test section, and the second image, taken during the period of steady flow over the test object (see Figures 2b and 3b), are taken as the input for the code to compare. Not much difference can be seen with the naked eye between the two images of the same model.

The main program for image processing, called a few functions for the purpose of performing the cross correlation initially and then for the process of integrating and filtering the density gradient function. First of all, the two images to be analysed were read and converted to a greyscale image in the Hue Saturation Value format. These images were filtered using a non-linear rank filter called the median filter. This filtering process performed the function of replacing each pixel with the median value of those in its neighbourhood.

The region of interest, which is the region in which we expect the flow to be present, was cut out from the original reference image. A function was then used to determine if there was any shift between the two input images due to movement of either the camera or the background pattern or both, between

the reference image and the flow image (see Figure 2c). The function determined the shift in terms of the number of pixels in the x and y directions. The code employed a cross-correlation algorithm, which in turn employed 2 D fast Fourier transforms, to determine the correlation between the two input images. The output of the function was in the form of number of pixels shift in the x and/or y direction. If there was any shift detected, one of the images was moved by a distance by which it had shifted to align the two images together. An image depicting the absolute difference (see Figure 2d and 3c) of the aligned images above was generated.

The next function called by the main program, was to derive vector style displacements for the density field (see Figures 2e and 3d). This code created a sliding template, which moved all over the window representing the region of interest, hence correlating and determining the correlation peak for each sub-window. The determination of correlation peak enabled us to compute the pattern shift based on the correlation peak position. The correlation peak was determined using the Gaussian peak fit. The result from this plot was in the form of a vector plot, which gave the magnitude and direction of the displacement vectors according to their positions.

The last function call executed by the main program performed the function of integrating the displacement vector field and providing us with a integrated potential which is the density distribution function. It solves the BOS problem using the direct differentiation formula. The result of the integrated potential is processed with the median filter again to get a filtered density field distribution image. The final BOS images for the cone and the Muses-C models are shown in figures 2f and 3e respectively. The intensity of light at each point in the processed image is a function of the density at that point, however no attempt has been made to quantify the density field at this stage.

For the tests with the cone model as the test object, the shock angles measured from the processed images match within 0.5° of the theoretically calculated values from the Taylor-Maccoll flow theory¹⁹. This theory solves for a calorically perfect flow field between a cone and a fore-body shock wave. For the axisymmetric flow around the model, the density distribution as displayed in regions above and below the centreline of the model appears to be very symmetric (see Figure 2f), as expected. Note however, that some repeat shots and shots at other conditions did not always display such good symmetry. The source of this lack of symmetry in some shots has not yet been identified. The processed image compared well (see Figure 2g) with a simulation performed using MB_CNS, a Navier-

Stokes solver for simulating two dimensional transient gas dynamics²⁰.

For the experiments with model of the Muses C re-entry capsule, standoff distances could be measured from processed BOS images. Typical value of standoff distance along the axial centerline was measured to be 2.5 ± 0.1 mm. Here again, the flow is symmetric around the axisymmetric model, with both the top and the bottom regions in the image around the re-entry body displaying similar patterns of density distribution.

At this stage, the results are only a qualitative experimental visualization of the density distribution. Future work is planned to apply an analytical treatment to quantify the density distributions.

Conclusions

The current set of experiments have demonstrated that the Background Oriented Schlieren technique can be successfully applied to visualize supersonic flow at Mach 4 in shock tunnels.

The shock shapes clearly identified the detached bow shock wave in case of the re-entry body and the attached oblique shock wave in the case of the conical test object. Shock angles and shock standoff distances for the different conditions were calculated. The shock angles measured from the processed images were within 2% of the theoretical calculations and matched well with the results of the CFD simulations.

Further work would be directed towards determining the density distribution in the flow field quantitatively. This can be achieved by developing an algorithm that can ascertain the density at different regions in the processed image, with the help of values at regions of known density, such as at the exit plane of the nozzle.

References

- ¹ H. Richard and M. Raffel (2001) *Principle and applications of the background oriented schlieren (BOS) method*. Measurement Science and Technology Vol 12, p 1576 – 1585
- ² G. E. A. Meier (2002) *Computerized background-oriented schlieren*. Experiments in Fluids Vol. 33, p 181 – 187
- ³ G. E. Elsinga, B. W. van Oudhuesden, F. Scarano and D.W. Watt (2004) *Assessment and application of quantitative schlieren methods: Calibrated color schlieren and background oriented schlieren*. Experiments in Fluids Vol. 36, p 309 – 325

- ⁴ S. B. Dalziel, G. O. Hughes, B. R. Sutherland (1998) *Synthetic Schlieren*. In: Carlomagno GM (ed) Proceedings of the 8th International Symposium on Flow Visualization, Sorrento, Italy, 1-4 September 1998, ISBN 0 9533991 0 9 (CD-ROM).
- ⁵ S. B. Dalziel, G. O. Hughes, B. R. Sutherland (2000) *Whole-field density measurements by 'synthetic schlieren'*. Experiments in Fluids Vol. 28, p 322-335
- ⁶ W. Merzkirch (1974) *Flow visualization* (New York: Academic)
- ⁷ R J Goldstein (1983) *Fluid mechanics measurements*. Hemisphere, Washington, DC.
- ⁸ M. Raffel, C. Willert, J. Kompenhans (1998) *Particle Image Velocimetry: a practical guide*. Springer, Berlin Heidelberg New York
- ⁹ C.E. Willert and M. Gharib (1991) *Digital Particle Image Velocimetry*. Experiments in Fluids, Vol. 10, p 181-193
- ¹⁰ R. N. Bracewell (1978) *The Fourier transforms and its applications*. New York. McGraw-Hill. 2nd ed. ISBN 007007013X
- ¹¹ E. O. Brigham (1974) *The fast Fourier transform* Englewood Cliffs, N.J: Prentice-Hall. ISBN 013307496X
- ¹² L. Venkatakrisnan and G. E. A. Meier (2004) *Density measurements using the Background Oriented Schlieren technique*. Experiments in Fluids, Vol. 37, p 237 – 247.
- ¹³ W. Weng, G. Liao, W. Fan *An improved cross correlation method for (digital) particle image velocimetry*. State Key Laboratories of Fire Sciences. University of Science and Technology of China.
- ¹⁴ D. P. Hart (2000) *PIV error correction*. Experiments in Fluids Vol. 29, p 13-22
- ¹⁵ T. Roesgen (2003) *Optimal subpixel interpolation in particle image velocimetry*. Experiments in Fluids Vol. 35, p 252-256
- ¹⁶ J. M. Austin, P.A. Jacobs, M.C, Kong, P. Barker, B.N. Littleton, and R. Gammie (1997) *The Small Shock Tunnel Facility at UQ*. Department of Mechanical Engineering Report 2/97. July 1997.
- ¹⁷ R.M. Krek and P.A. Jacobs (1993) *STN, Shock Tube and Nozzle Calculations for equilibrium air*. Department of Mechanical Engineering Report 2/93. February 1997.
- ¹⁸ The Institute of Space and Astronautical Science. URL: www.muses-c.isas.ac.jp. Japan Aerospace Exploration Agency.
- ¹⁹ G. I. Taylor and J. W. Maccoll (1933) *The air pressure on a cone moving at high speeds, I and II*. Proceedings of the Royal Society of London, Series A, Vol. 139, No. 838, p 278 – 311.
- ²⁰ P.A. Jacobs (1996) *MB CNS, a computer program for the simulation of transient compressible flow*. Department of Mechanical Engineering Report 10/96, The University of Queensland, Brisbane, Australia.

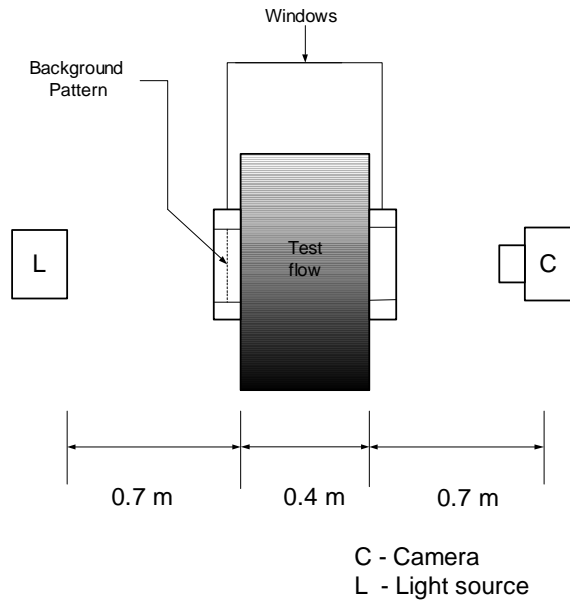
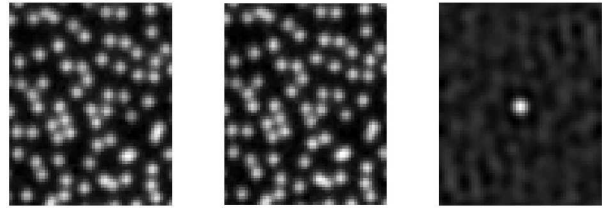
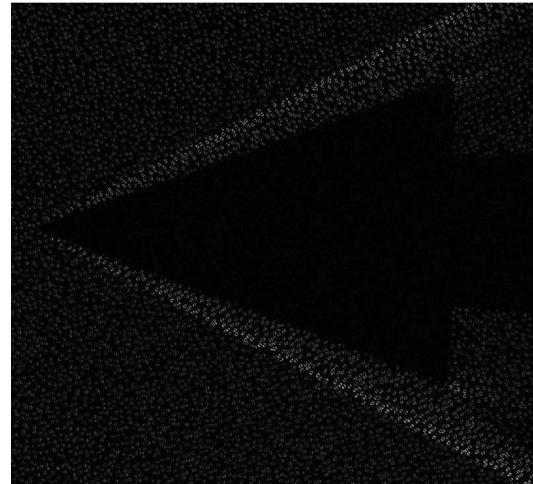


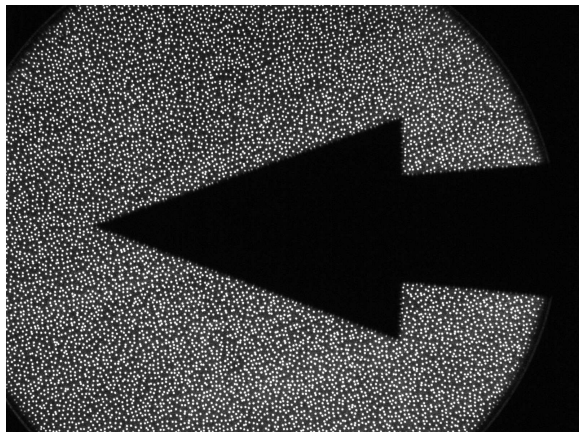
Figure 1: A schematic of the BOS setup for our experiments



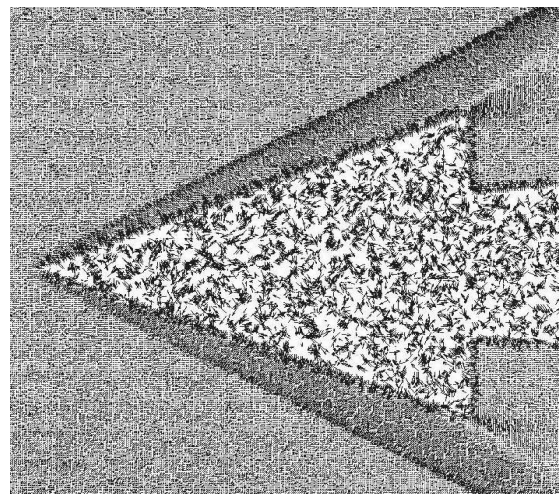
2 (c) Global correlation peak to detect any shifts between the two images



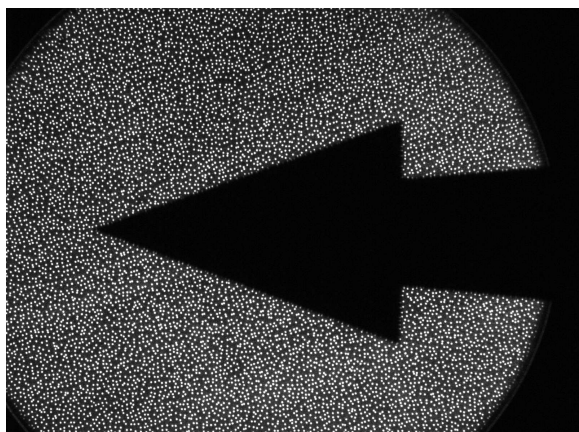
2 (d) Absolute difference, for a quick look analysis



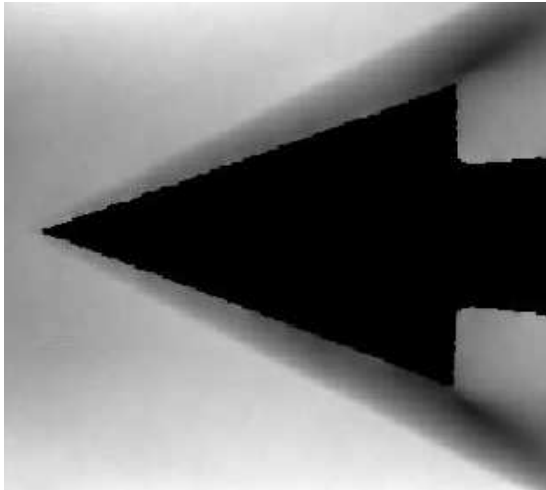
2 (a) Reference image in quiescent gas



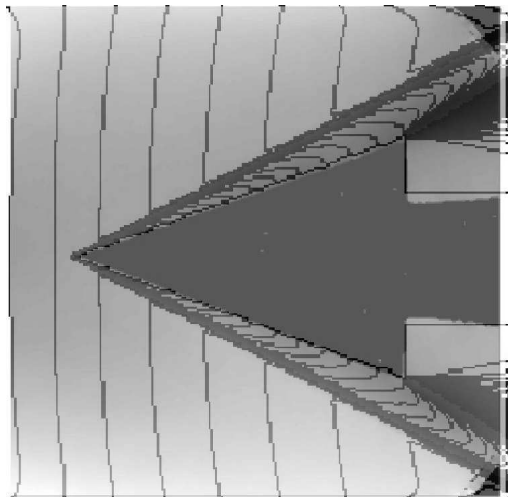
2 (e) Vector displacement, representing density gradients in the region



2 (b) Image with flow established in the test section

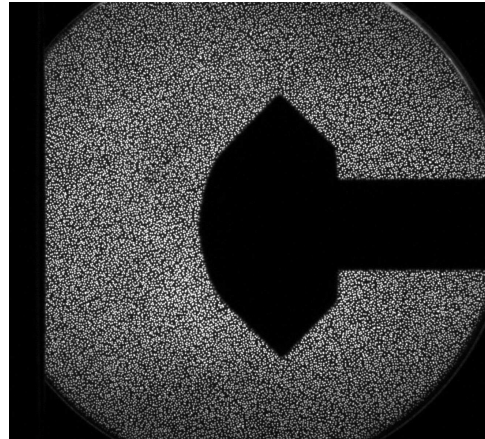


2 (f) The density distribution plot, representing the density distribution in the test section.

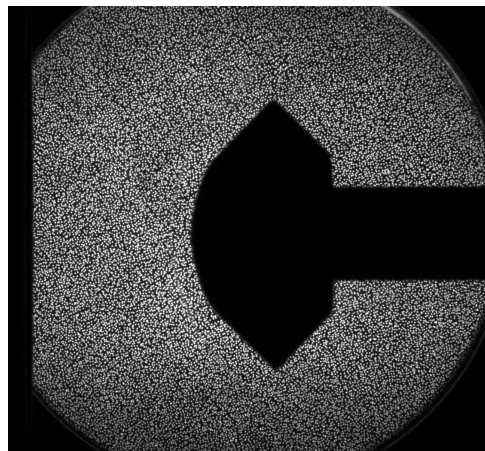


2 (g) CFD simulation result superimposed onto the processed image.

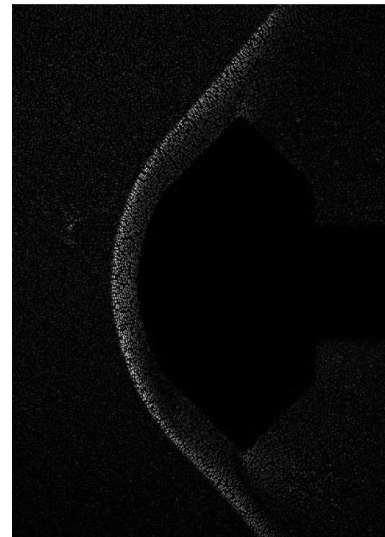
Figure 2: Raw and processed images for the 20° semi-vertex angle circular cone model. For 15 kPa shock tube fill pressure.



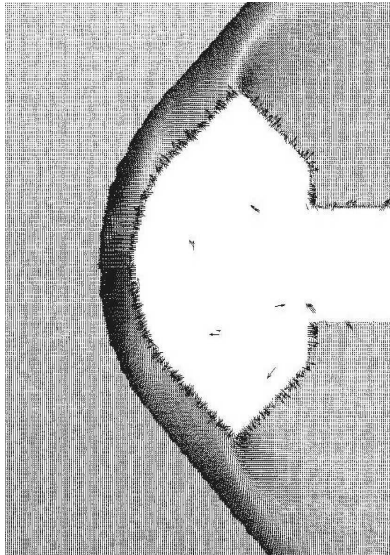
3 (a) Reference image in quiescent gas



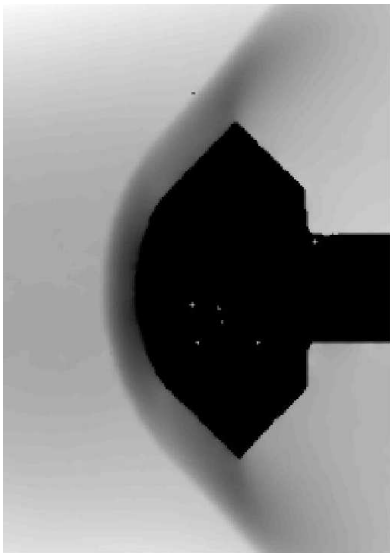
3 (b) Image with flow established in the test section



3 (c) Absolute difference, for a quick look analysis



3 (d) Vector displacement, representing density gradients in the region



3 (e) The density distribution plot representing the density distribution in the test section.

Figure 3: Raw and processed images for the Muses C re-entry capsule model. For 15 kPa shock tube fill pressure.